

Rare Earth-rich Magnesium Compounds RE_4RhMg ($RE = Y, La-Nd, Sm, Gd-Tm, Lu$)

Selcan Tuncel^a, Ute Ch. Rodewald^a, Bernard Chevalier^b, and Rainer Pöttgen^a

^a Institut für Anorganische und Analytische Chemie, Westfälische Wilhelms-Universität Münster, Corrensstraße 30, 48149 Münster, Germany

^b Institut de Chimie de la Matière Condensée de Bordeaux (ICMCB), CNRS [UPR 9048], Université Bordeaux 1, 87 avenue du Docteur Albert Schweitzer, 33608 Pessac Cedex, France

Reprint requests to R. Pöttgen. E-mail: pottgen@uni-muenster.de

Z. Naturforsch. **2007**, 62b, 642–646; received December 20, 2006

The series of magnesium compounds RE_4RhMg ($RE = Y, La-Nd, Sm, Gd-Tm, Lu$) was prepared by high-frequency melting of the elements in sealed tantalum tubes. All samples were investigated by powder X-ray diffraction. The structures with $RE = Sm, Gd, Dy, Ho$, and Er as rare earth metal components were refined from single crystal diffractometer data: Gd_4RhIn -type, $F\bar{4}3m$, $Z = 16$, $a = 1392.1(1)$ pm, $wR2 = 0.060$, 616 F^2 values, 19 variables for Sm_4RhMg , $a = 1380.8(2)$ pm, $wR2 = 0.071$, 530 F^2 values, 19 variables for Gd_4RhMg , $a = 1366.9(1)$ pm, $wR2 = 0.070$, 594 F^2 values, 20 variables for Dy_4RhMg , $a = 1355.7(2)$ pm, $wR2 = 0.077$, 578 F^2 values, 20 variables for $Ho_{3.52}RhMg_{1.48}$, and $a = 1355.4(2)$ pm, $wR2 = 0.075$, 559 F^2 values, 20 variables for $Er_{3.94}RhMg_{1.06}$. The rhodium atoms have slightly distorted trigonal prismatic rare earth coordination. Condensation of the $RhRE_6$ prisms leads to a three-dimensional network which leaves large voids that are filled by regular Mg_4 tetrahedra with a $Mg-Mg$ distance of 312 pm in Sm_4RhMg . The magnesium atoms have twelve nearest neighbors (3 $Mg + 9 RE$) in icosahedral coordination. In the structures with holmium and erbium, the $RE1$ positions which are not involved in the trigonal prismatic network exhibit $RE1/Mg$ mixing. Shortest distances occur for $Sm-Rh$ (286 pm) within the rigid three-dimensional network of condensed trigonal prisms.

Key words: Magnesium, Intermetallics, Crystal Chemistry

Introduction

Among the many rare earth (RE)-transition metal (T)-magnesium compounds, those with nickel as the transition metal component have most intensively been investigated with respect to crystal chemistry and hydrogenation behavior [1–22]. These materials are under discussion for hydrogen storage applications. Besides the well ordered nickel based compounds RE_4NiMg [23], RE_2Ni_2Mg [1, 5, 6], $RENi_4Mg$ [7, 8, 12], $RENi_9Mg_2$ [2–4], $LaNiMg_2$ [9, 15], also a variety of metallic glasses [24] and ball-milled (mechanosynthesis) [25] materials have been reported.

Less information is available on the cobalt and rhodium based materials. So far, only the series $RE_4Co_2Mg_3$ ($RE = Pr, Nd, Sm, Gd, Tb, Dy$) [26, 27], RE_4CoMg [28], and $RERhMg$ ($RE = La, Ce, Pr, Nd$) [29] are known. We have started systematic phase analytical studies of the $RE-T-Mg$ systems and have now obtained new intermetallics RE_4RhMg ($RE = Y, La-Nd, Sm, Gd-Tm, Lu$) with cubic Gd_4RhIn -type

structure. The synthesis and crystal chemistry of these compounds are reported herein.

Experimental Section

Synthesis

Starting materials for the preparation of the RE_4RhMg samples were ingots of the rare earth metals (Johnson Matthey, > 99.9%), rhodium powder (Degussa-Hüls, 200 mesh, > 99.9%), and a magnesium rod (Johnson Matthey, \varnothing 16 mm, > 99.95%). The surface of the magnesium rod was cut on a turning lathe in order to remove surface impurities. The elements were weighed in the ideal 4:1:1 atomic ratio and arc-welded [30] in tantalum ampoules under an argon pressure of ca. 600 mbar. The argon was purified before over molecular sieves, silica gel and titanium sponge (900 K). The ampoules were then placed in a water-cooled quartz sample chamber [31] of an induction furnace (Hüttinger Elektronik, Freiburg, Typ TIG 1.5/300), first heated for 2 min at ca. 1300 K and subsequently annealed for another 2 h at ca. 920 K, followed by rapid cooling within the sample chamber. The temperature was controlled

through a Sensor Therm Metis MS09 pyrometer with an accuracy of ± 30 K. The brittle reaction products could easily be separated from the ampoules. No reaction with the tantalum container was evident. All polycrystalline RE_4RhMg samples are light gray and stable in air over months. Single crystals exhibit metallic luster.

The single crystals investigated on the diffractometer and the bulk samples were analyzed by EDX in a LEICA 420 I scanning electron microscope using the lanthanoid trifluorides, rhodium, and magnesium oxide as standards. The semiquantitative EDX analyses revealed no impurity elements and were in agreement with the ideal 4 : 1 : 1 composition. The $Ho_{3.52}RhMg_{1.48}$ crystal revealed a smaller holmium content in agreement with the structure refinement.

X-Ray powder and single crystal data

The polycrystalline RE_4RhMg samples were investigated through their Guinier powder patterns using $CuK\alpha_1$ radiation and α -quartz ($a = 491.30$ and $c = 540.46$ pm) as an internal standard. The Guinier camera was equipped with an imaging plate system (Fujifilm BAS-1800). The cubic lattice parameters (Table 1) were obtained from least-squares refinements of the Guinier data. The correct indexing was ensured through intensity calculations [32] using the atomic positions obtained from the structure refinements. While the single crystal lattice parameters of Sm_4RhMg , Gd_4RhMg , and Dy_4RhMg agreed well with the powder data, the $Ho_{3.52}RhMg_{1.48}$ and $Er_{3.94}RhMg_{1.06}$ single crystals revealed a smaller a parameter as compared to the powder (Table 1).

Most of the RE_4RhMg samples were well crystallized. Single crystals were selected from the Sm, Gd, Dy, Ho, and Er containing samples and first examined by Laue photographs on a Buerger precession camera (equipped with an imaging plate system Fujifilm BAS-1800) in order to establish the crystal quality. Single crystal intensity data of Gd_4RhMg were collected at r.t. on a Nonius CAD4 four-circle diffractometer with graphite monochromatized $MoK\alpha$ radiation (71.073 pm) and a scintillation counter with pulse height discrimination. The scans were performed in the $\omega/2\theta$ mode. Empirical absorption corrections were applied on the basis of Ψ scan data followed by spherical absorption corrections. Intensity data of the remaining crystals were collected in oscillation mode on a Stoe IPDS-II image plate diffractometer using monochromatized $MoK\alpha$ radiation (71.073 pm). Numerical absorption corrections were applied to these data sets. All relevant crystallographic data and details for the data collections and evaluations are listed in Table 2.

Isotropy of the RE_4RhMg compounds with the cubic Gd_4RhIn -type [33, 34] was already evident from the powder data, and the systematic extinctions of the data sets were compatible with space group $F\bar{4}3m$. The atomic posi-

Table 1. Lattice parameters (Guinier powder data) of the ternary magnesium compounds RE_4RhMg .

| Compound | a (pm) | V (nm ³) |
|--------------------------|-----------|------------------------|
| Y_4RhMg | 1377.0(2) | 2.6109 |
| La_4RhMg | 1437.1(1) | 2.9679 |
| Ce_4RhMg | 1417.5(1) | 2.8484 |
| Pr_4RhMg | 1415.1(5) | 2.8335 |
| Nd_4RhMg | 1405.9(2) | 2.7786 |
| Sm_4RhMg | 1392.1(1) | 2.6979 |
| Gd_4RhMg | 1380.8(2) | 2.6328 |
| Tb_4RhMg | 1377.7(2) | 2.5751 |
| Dy_4RhMg | 1366.9(1) | 2.5537 |
| Ho_4RhMg | 1362.3(1) | 2.5283 |
| $Ho_{3.52}RhMg_{1.48}^*$ | 1355.7(2) | 2.4917 |
| Er_4RhMg | 1358.2(1) | 2.5054 |
| $Er_{3.94}RhMg_{1.06}^*$ | 1355.4(2) | 2.4900 |
| Tm_4RhMg | 1350.8(1) | 2.4648 |
| Lu_4RhMg | 1348.1(1) | 2.4498 |

* single crystal data.

tions of Gd_4RhIn were then taken as starting values and the structures were refined using SHELXL-97 (full-matrix least-squares on F_o^2) [35] with anisotropic atomic displacement parameters for all sites. As a check for possible defects or mixed occupied sites, the occupancy parameters were refined in a separate series of least-squares cycles. For Sm_4RhMg , Gd_4RhMg , and Dy_4RhMg all sites were fully occupied within two standard uncertainties. The crystals with holmium and erbium revealed significant $RE1/Mg$ mixing, leading to the compositions $Ho_{3.52}RhMg_{1.48}$ and $Er_{3.94}RhMg_{1.06}$ for the investigated crystals. Refinement of the correct absolute structure was ensured through refinement of the Flack parameters [36, 37]. Only the Dy_4RhMg crystal showed twinning by inversion. Final difference Fourier syntheses revealed no significant residual peaks (see Table 2). The positional parameters and interatomic distances are listed in Tables 3 and 4. Further details on the structure refinements are available.*

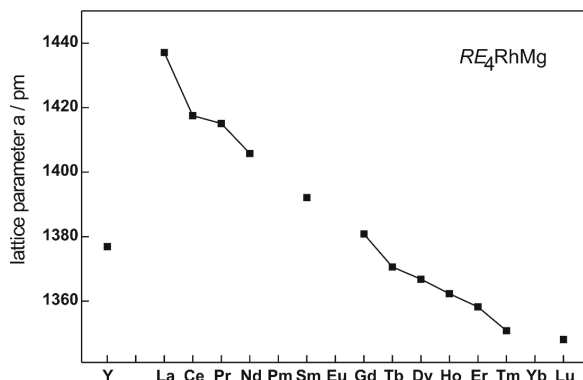
Discussion

The magnesium compounds RE_4RhMg ($RE = Y$, La–Nd, Sm, Gd–Tm, Lu) crystallize with the cubic Gd_4RhIn -type [33, 34] structure. The cell volume (Table 1 and Fig. 1) decreases from the lanthanum to the lutetium compound as expected from the lanthanoid contraction. The volume of the yttrium compound fits in between the volumes of the gadolinium and the terbium compound, similar to the series of isotypic RE_4CoMg compounds [28]. A small anomaly is evi-

*Details may be obtained from: Fachinformationszentrum Karlsruhe, D-76344 Eggenstein-Leopoldshafen (Germany), by quoting the Registry No's. CSD-417452 (Sm_4RhMg), CSD-417453 (Gd_4RhMg), CSD-417454 (Dy_4RhMg), CSD-417455 ($Ho_{3.52}RhMg_{1.48}$), and CSD-417456 ($Er_{3.94}RhMg_{1.06}$).

Table 2. Crystal data and structure refinement for RE_4RhMg , Gd_4RhIn -type, space group $F\bar{4}3m$, $Z = 16$.

| Empirical formula | Sm_4RhMg | Gd_4RhMg | Dy_4RhMg | $Ho_{3.52}RhMg_{1.48}$ | $Er_{3.94}RhMg_{1.06}$ |
|---|-------------------------------|-------------------------------|-------------------------------|-------------------------------|-------------------------------|
| Molar mass [g/mol] | 728.62 | 756.22 | 777.22 | 718.92 | 786.97 |
| Unit cell dimensions | Table 1 | Table 1 | Table 1 | Table 1 | Table 1 |
| Calculated density [g/cm ³] | 7.18 | 7.63 | 8.09 | 7.67 | 8.40 |
| Crystal size [μm^3] | $20 \times 50 \times 50$ | $10 \times 30 \times 40$ | $20 \times 70 \times 80$ | $20 \times 30 \times 50$ | $20 \times 30 \times 90$ |
| Detector distance [mm] | 60 | — | 60 | 60 | 60 |
| Exposure time [min] | 5 | — | 4 | 5 | 5 |
| ω range; increment [°] | 0–180; 1.0 | — | 0–180; 1.0 | 0–180; 1.0 | 0–180; 1.0 |
| Integr. param. A, B, EMS | 13.5; 3.5; 0.012 | — | 13.5; 3.5; 0.012 | 13.5; 3.5; 0.012 | 13.5; 3.5; 0.012 |
| Transm. ratio (max/min) | 2.64 | 4.58 | 2.46 | 1.44 | 2.88 |
| Absorption coefficient [mm ⁻¹] | 36.6 | 42.2 | 48.7 | 46.7 | 55.0 |
| $F(000)$ | 4880 | 5008 | 5136 | 4774 | 5206 |
| θ range [°] | 2 to 35 | 2 to 33 | 2 to 35 | 2 to 35 | 3 to 35 |
| Range in hkl | $\pm 22, \pm 22, \pm 22$ | $\pm 20, \pm 20, \pm 20$ | $\pm 21, \pm 21, \pm 21$ | $\pm 21, \pm 21, \pm 21$ | $\pm 21, \pm 21, \pm 21$ |
| Total no. reflections | 9953 | 5337 | 9534 | 9245 | 5291 |
| Independent reflections (R_{int}) | 616 (0.060) | 530 (0.135) | 594 (0.142) | 578 (0.156) | 559 (0.084) |
| Reflections with $I \geq 2\sigma(I)$ (R_σ) | 552 (0.032) | 460 (0.052) | 543 (0.052) | 433 (0.079) | 455 (0.059) |
| Data/parameters | 616 / 19 | 530 / 19 | 594 / 20 | 578 / 20 | 559 / 20 |
| Goodness-of-fit on F^2 | 1.119 | 1.056 | 1.089 | 0.885 | 0.912 |
| Final R indices [$I \geq 2\sigma(I)$] | $R1 = 0.031$ $wR2 = 0.059$ | $R1 = 0.031$ $wR2 = 0.068$ | $R1 = 0.031$ $wR2 = 0.070$ | $R1 = 0.040$ $wR2 = 0.075$ | $R1 = 0.035$ $wR2 = 0.073$ |
| R indices (all data) | $R1 = 0.037$ $wR2 = 0.060$ | $R1 = 0.039$ $wR2 = 0.071$ | $R1 = 0.035$ $wR2 = 0.070$ | $R1 = 0.057$ $wR2 = 0.077$ | $R1 = 0.044$ $wR2 = 0.075$ |
| Extinction coefficient | 0.00014(1) | 0.000034(9) | 0.00018(2) | 0.00016(2) | 0.00015(1) |
| Flack parameter | 0.05(5) | −0.05(5) | — | −0.01(6) | −0.04(5) |
| BASF | — | — | 0.20(4) | — | — |
| Largest diff. peak and hole [e/Å ³] | 2.51 / −2.17 | 1.61 / −1.53 | 3.47 / −2.29 | 2.16 / −2.83 | 3.04 / −3.59 |

Fig. 1. Course of the unit cell volumes in the series RE_4RhMg .

dent for Ce_4RhMg . The cell volume is slightly smaller than expected, most likely indicating a tendency for intermediate valence cerium. Detailed property investigations are in progress.

As an example we discuss the samarium compound. The Sm_4RhMg structure contains three crystallographically independent samarium sites, one rhodium, and one magnesium site. The rhodium atoms have slightly distorted trigonal prismatic coordination of the $Sm2$ and $Sm3$ atoms. These trigonal prisms are

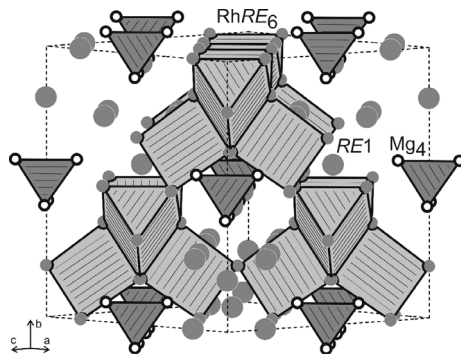


Fig. 2. View of the RE_4RhMg crystal structure. Rare earth, rhodium, and magnesium atoms are drawn as medium grey, filled (hidden in the trigonal prisms), and open circles, respectively. The three-dimensional network of corner-sharing $RhRE_6$ trigonal prisms and the Mg_4 tetrahedra are emphasized. The $RE1$ atoms do not participate in the network of condensed trigonal prisms.

condensed *via* all corners leading to a rigid three-dimensional network (Fig. 2). The $RE1$ atoms do not directly belong to the network. However, they are capping the $RhRE_2RE_3$ prisms on the rectangular faces, but at much longer $RE1$ –Rh distances (see Table 4). The shorter $RE2$ –Rh and $RE3$ –Rh distances of 286 pm are slightly smaller than the sum of the

Table 3. Atomic coordinates and isotropic displacement parameters (pm^2) of RE_4RhMg . U_{eq} is defined as one third of the trace of the orthogonalized U_{ij} tensor.

| Atom | Wyckoff site | x | y | z | U_{eq} |
|---|--------------|------------|-----|-----|----------|
| <i>Sm₄RhMg</i> | | | | | |
| Sm1 | 24g | 0.56400(6) | 1/4 | 1/4 | 109(2) |
| Sm2 | 24f | 0.18798(6) | 0 | 0 | 85(2) |
| Sm3 | 16e | 0.34644(4) | x | x | 80(2) |
| Rh | 16e | 0.14164(6) | x | x | 109(3) |
| Mg | 16e | 0.5793(3) | x | x | 72(11) |
| <i>Gd₄RhMg</i> | | | | | |
| Gd1 | 24g | 0.56450(7) | 1/4 | 1/4 | 183(2) |
| Gd2 | 24f | 0.18789(7) | 0 | 0 | 159(2) |
| Gd3 | 16e | 0.34635(5) | x | x | 156(2) |
| Rh | 16e | 0.14172(8) | x | x | 186(4) |
| Mg | 16e | 0.5794(3) | x | x | 174(15) |
| <i>Dy₄RhMg</i> | | | | | |
| Dy1 | 24g | 0.56445(6) | 1/4 | 1/4 | 120(2) |
| Dy2 | 24f | 0.18771(6) | 0 | 0 | 92(2) |
| Dy3 | 16e | 0.34660(4) | x | x | 93(2) |
| Rh | 16e | 0.14173(7) | x | x | 129(3) |
| Mg | 16e | 0.5797(3) | x | x | 84(11) |
| <i>Ho_{3.52}RhMg_{1.48}</i> | | | | | |
| 67.8(8) % Ho1/32.2(2) % Mg2 | 24g | 0.4359(1) | 3/4 | 3/4 | 114(5) |
| Ho2 | 24f | 0.81002(8) | 0 | 0 | 101(3) |
| Ho3 | 16e | 0.65356(6) | x | x | 89(3) |
| Rh | 16e | 0.8592(1) | x | x | 151(5) |
| Mg1 | 16e | 0.4189(5) | x | x | 112(20) |
| <i>Er_{3.94}RhMg_{1.06}</i> | | | | | |
| 95.7(10) % Er1/4.3(10) % Mg2 | 24g | 0.43560(8) | 3/4 | 3/4 | 93(3) |
| Er2 | 24f | 0.81213(8) | 0 | 0 | 75(2) |
| Er3 | 16e | 0.65344(6) | x | x | 78(3) |
| Rh | 16e | 0.8583(1) | x | x | 117(5) |
| Mg1 | 16e | 0.4209(4) | x | x | 60(19) |

covalent radii (291 pm) [38], and we can assume strong RE –Rh bonding. This is in excellent agreement with recent electronic structure calculations on isotopic La_4CoMg [28]. A striking structural motif is the regular Mg_4 tetrahedron which is located on all edges of the unit cell (Fig. 2). The edge length of 312 pm is smaller than the average Mg–Mg distance of 320 pm in *hcp* magnesium [39].

Finally we need to comment on the homogeneity ranges within the family of RE_4RhMg compounds. The single crystal data of the holmium and the erbium

Table 4. Interatomic distances (pm), calculated with the powder lattice parameters of Sm_4RhMg . Standard deviations are given in parentheses. All distances within the first coordination spheres are listed.

| | | | | | | | |
|------|---|-----|----------|------|---|-----|----------|
| Sm1: | 2 | Mg | 336.7(5) | Sm3: | 3 | Rh | 286.1(1) |
| | 2 | Rh | 357.0(1) | | 3 | Mg | 355.6(2) |
| | 2 | Sm3 | 357.5(1) | | 3 | Sm1 | 357.5(1) |
| | 4 | Sm1 | 366.2(1) | | 3 | Sm2 | 374.3(1) |
| | 4 | Sm2 | 369.5(1) | | 3 | Sm3 | 379.7(2) |
| Sm2: | 2 | Rh | 286.2(1) | Rh: | 3 | Sm3 | 286.1(1) |
| | 2 | Mg | 359.6(1) | | 3 | Sm2 | 286.2(2) |
| | 4 | Sm1 | 369.5(1) | | 3 | Sm1 | 357.0(1) |
| | 4 | Sm2 | 370.1(1) | Mg: | 3 | Mg | 312(1) |
| | 2 | Sm3 | 374.3(1) | | 3 | Sm1 | 336.7(5) |
| | | | | | 3 | Sm3 | 355.6(2) |
| | | | | | 3 | Sm2 | 359.6(1) |

compound revealed substantial $RE1/Mg$ mixing, leading to the compositions $Ho_{3.52}RhMg_{1.48}$ and $Er_{3.94}RhMg_{1.06}$ for the investigated single crystals. Similar behaviour was also observed in the cobalt based series, especially for the crystal of composition $Dy_{3.27(1)}CoMg_{1.73(1)}$ [28], while no $RE1/Cd$ mixing was detected for the cadmium compounds RE_4CoCd and RE_4RhCd ($RE = Tb, Dy, Ho$) [40]. So far, $RE1/Mg$ mixing has only been observed for the compounds with the late rare earth elements, probably due to geometric constraints, since the metallic radius of magnesium (160 pm [38]) is only comparable with the smaller rare earth elements (*e.g.* 176 pm for erbium [38]). Substitution of the rare earth element by the smaller magnesium atoms leads to a drastic decrease of the a lattice parameter (Table 1). The $RE_{4-x}CoMg_{1+x}$ and $RE_{4-x}RhMg_{1+x}$ solid solutions are therefore highly interesting from a magnetic point of view. Detailed magnetization and neutron diffraction studies on selected compounds are in progress.

Acknowledgements

We thank Dipl.-Chem. F.M. Schappacher for the work at the scanning electron microscope. This work was financially supported by the Deutsche Forschungsgemeinschaft. B.C. and R.P. are indebted to EGIDE and DAAD for research grants within the PROCOPE programs (11457RD and D/0502176).

- [1] C. Geibel, U. Klinger, M. Weiden, B. Buschinger, F. Steglich, *Physica B* **1997**, 237–238, 202.
- [2] K. Kadir, T. Sakai, I. Uehara, *J. Alloys Compd.* **1997**, 257, 115.

- [3] K. Kadir, T. Sakai, I. Uehara, *J. Alloys Compd.* **1999**, 287, 264.
- [4] K. Kadir, T. Sakai, I. Uehara, *J. Alloys Compd.* **2000**, 302, 112.

- [5] R. Pöttgen, A. Fugmann, R.-D. Hoffmann, U. Ch. Rodewald, D. Niepmann, *Z. Naturforsch.* **2000**, 55b, 155.
- [6] R.-D. Hoffmann, A. Fugmann, U. Ch. Rodewald, R. Pöttgen, *Z. Anorg. Allg. Chem.* **2000**, 626, 1733.
- [7] K. Kadir, D. Noéus, I. Yamashita, *J. Alloys Compd.* **2002**, 345, 140.
- [8] L. Guénée, V. Favre-Nicolin, K. Yvon, *J. Alloys Compd.* **2003**, 348, 129.
- [9] G. Renaudin, L. Guénée, K. Yvon, *J. Alloys Compd.* **2003**, 350, 145.
- [10] Z. L. Wang, H. Y. Zhou, Z. F. Gu, G. Cheng, A. B. Yu, *J. Alloys Compd.* **2004**, 377, L7.
- [11] Z. M. Wang, H. Y. Zhou, Z. F. Gu, G. Cheng, A. B. Yu, *J. Alloys Compd.* **2004**, 381, 234.
- [12] Z. M. Wang, H. Y. Zhou, G. Cheng, Z. F. Gu, A. B. Yu, *J. Alloys Compd.* **2004**, 384, 279.
- [13] Z. Huaiying, X. Xin, Ch. Gang, W. Zhongmin, Zh. Songli, *J. Alloys Compd.* **2005**, 386, 144.
- [14] S. De Negri, M. Giovannini, A. Saccone, *J. Alloys Compd.* **2005**, 397, 126.
- [15] A. Doğan, D. Johrendt, R. Pöttgen, *Z. Anorg. Allg. Chem.* **2005**, 631, 451.
- [16] K. Yvon, G. Renaudin, C. M. Wei, M. Y. Chou, *Phys. Rev. Lett.* **2005**, 94, 066403.
- [17] H. Zhou, Zh. Wang, Q. Yao, *J. Alloys Compd.* **2006**, 407, 129.
- [18] Q. Yao, H. Zhou, Zh. Wang, *J. Alloys Compd.* **2006**, 421, 117.
- [19] L. J. Huang, G. Y. Liang, Z. B. Sun, *J. Alloys Compd.* **2006**, 421, 279.
- [20] F. Zhang, Y. Luo, K. Sun, D. Wang, R. Yan, L. Kang, J. Chen, *J. Alloys Compd.* **2006**, 424, 218.
- [21] F.-L. Zhang, Y.-Ch. Luo, J.-P. Chen, R.-X. Yan, J.-H. Chen, *J. Alloys Compd.* **2006**, 430, 302.
- [22] S. De Negri, M. Giovannini, A. Saccone, *J. Alloys Compd.* **2007**, in press.
- [23] S. Tuncel, B. Chevalier, J.-L. Bobet, E. Gaudin, R. Pöttgen, unpublished results.
- [24] T. Spassov, V. Rangelova, N. Neykov, *J. Alloys Compd.* **2002**, 334, 219.
- [25] M. Zhu, C. H. Peng, L. Z. Ouyang, T. Q. Tong, *J. Alloys Compd.* **2006**, 426, 316.
- [26] S. Tuncel, R.-D. Hoffmann, B. Heying, B. Chevalier, R. Pöttgen, *Z. Anorg. Allg. Chem.* **2006**, 632, 2017.
- [27] S. Tuncel, U. Ch. Rodewald, S. F. Matar, B. Chevalier, R. Pöttgen, *Z. Naturforsch.* **2007**, 62b, 162.
- [28] S. Tuncel, R.-D. Hoffmann, B. Chevalier, S. F. Matar, R. Pöttgen, *Z. Anorg. Allg. Chem.* **2007**, 633, 151.
- [29] Th. Fickenscher, R.-D. Hoffmann, R. Kraft, R. Pöttgen, *Z. Anorg. Allg. Chem.* **2002**, 628, 667.
- [30] R. Pöttgen, Th. Gulden, A. Simon, *GIT Labor Fachzeitschrift* **1999**, 43, 133.
- [31] D. Kußmann, R.-D. Hoffmann, R. Pöttgen, *Z. Anorg., Allg. Chem.* **1998**, 624, 1727.
- [32] K. Yvon, W. Jeitschko, E. Parthé, *J. Appl. Crystallogr.* **1977**, 10, 73.
- [33] R. Zaremba, U. Ch. Rodewald, R. Pöttgen, *Z. Kristallogr.* **2006**, Suppl. 14, 161.
- [34] R. Zaremba, U. Ch. Rodewald, R. Pöttgen, *Z. Anorg. Allg. Chem.* **2006**, 632, 2106.
- [35] G. M. Sheldrick, SHELXL-97, Program for the Refinement of Crystal Structures, University of Göttingen, Göttingen (Germany) **1997**.
- [36] H. D. Flack, G. Bernadinelli, *Acta Crystallogr.* **1999**, A55, 908.
- [37] H. D. Flack, G. Bernadinelli, *J. Appl. Crystallogr.* **2000**, 33, 1143.
- [38] J. Emsley, *The Elements*, Oxford University Press, Oxford (U. K.) **1999**.
- [39] J. Donohue, *The Structures of the Elements*, Wiley, New York (USA) **1974**.
- [40] A. Doğan, S. Rayaprol, R. Pöttgen, *J. Phys.: Condens. Matter*, **2007**, 19, 076213.